N-GLYCOSYLATION-DEPENDENT CONTROL OF FUNCTIONAL EXPRESSION OF BACKGROUND POTASSIUM CHANNELS $K_{2P}3.1$ AND $K_{2P}9.1$

Alexandra Mant, Sarah Williams, Laura Roncoroni, Eleanor Lowry¹, Daniel Johnson¹ and Ita O'Kelly

From Human Development and Health, Centre for Human Development, Stem Cells and Regeneration, University of Southampton, Southampton, SO16 6YD, UK

¹Faculty of Life Sciences, University of Manchester, Manchester, M13 9PT, UK

Running head: Glycosylation of TASK channels

Address correspondence to: Dr I. O'Kelly, Human Development and Health, Duthie Building, Mail Point 808, University of Southampton, Southampton SO16 6YD. Tel: +44 23 8079 6421; Fax: +44 23 8079 4264; E-mail: I.M.O'Kelly@southampton.ac.uk

Keywords: K_{2P} channel, TASK, K⁺ channel, *N*-linked glycosylation, membrane targeting, trafficking, surface expression.

CAPSULE

Background *N*-glycosylation regulates the function of many membrane proteins **Results** $K_{2P}3.1$ and $K_{2P}9.1$ possess functional glycosylation sites and lack of glycosylation results in fewer channels on the cell surface **Conclusions** *N*-linked glycosylation has a critical role in $K_{2P}3.1$ and a modulatory role in $K_{2P}9.1$ cell surface expression.

Significance This defines a direct link between background potassium channel function and metabolic status.

SUMMARY

Two-pore domain potassium (K_{2P}) channels play fundamental roles in cellular processes by enabling a constitutive leak of potassium from cells in which they are expressed, thus influencing cellular membrane potential and activity. Hence, regulation of these channels is of critical importance to cellular function. A key regulatory mechanism of K_{2P} channels is the control of their cell surface expression. Membrane protein delivery to and retrieval from the cell surface is controlled by their passage through the secretory and endocytic pathways and post-translational modifications regulate their progression through these pathways. All but one of the K_{2P} channels possess consensus N-linked glycosylation sites and here we demonstrate that the conserved putative N-glycosylation site in K_{2P}3.1 and K_{2P}9.1 is a glycan acceptor site. Patch-clamp analysis revealed that disruption of channel glycosylation reduced K_{2P}3.1 current, and flow cytometry was instrumental in attributing this to a decreased number of channels on the cell surface. Similar findings were observed when cells were cultured in reduced glucose concentrations. **Disruption** of *N*-linked glycosylation has less effect on $K_{2P}9.1$, with a small reduction in number of channels on the surface observed, but no functional implications detected. As non-glycosylated channels appear to pass through the secretory pathway in a

manner comparable to glycosylated channels, evidence presented here suggests that the decreased number of non-glycosylated $K_{2P}3.1$ channels on the cell surface may be due to their decreased stability.

INTRODUCTION

Cellular membrane potential influences function of both excitable and non-excitable cells. The two-pore domain potassium (K_{2P}) channels are a family of background channels that regulate the membrane potential of cells in which they are expressed. Both structurally and functionally dissimilar to other potassium channel families, K_{2P} channels display little voltage or time dependence, are active at resting membrane potentials and allow a constitutive leak of K⁺ from cells [1,2]. The acid sensitive K_{2P} subgroup (TASK channels) includes two well-characterised members, K_{2P}3.1 (TASK-1) and $K_{2P}9.1$ (TASK-3), and a third proposed member (K_{2P}15.1 or TASK-5), which remains uncharacterised to date. Due to their cellular localisation and sensitivity physiological stimuli (extracellular acidification and hypoxia) TASK channels have implicated in an array of physiological processes including regulatory roles in cell proliferation (and oncogenesis), activation of T-cells, chemoreception as well as neuroprotective roles in response to ischemia and inflammation [3-5]. TASK channels are also molecular targets for both local anesthetics and endocannabinoids [3,6]. These channels show constitutive activity once expressed on the cell surface, hence the control of TASK channel surface expression is of critical importance, as any change in channel number at the plasma membrane impacts the electrical properties of the cell in which these channels are expressed.

Numerous in-built processes within the secretory pathway are employed to regulate delivery of correctly folded membrane proteins, in appropriate number, to the cell surface. We and others have previously shown that TASK channel phosphorylation and association with cytosolic adaptor protein, 14-3-3, is critical to $K_{2P}3.1$ and $K_{2P}9.1$ export from the endoplasmic reticulum (ER) and hence cell surface expression [7-10].

Understanding of the quality control processes newly synthesised proteins undergo en route to the cell surface is still developing. Key steps include retention of nascent proteins within the ER until correctly folded and assembled. removal of persistently misfolded proteins and transport of correctly folded proteins to the Golgi complex (GC). Further quality control together with protein maturation occurs within the Endoplasmic Reticulum-Golgi Intermediate Compartment (ERGIC) and GC, which ultimately leads to delivery of mature membrane proteins to the plasma membrane or removal of misfolded proteins to the endosomes and lysosomes [11,12].

Protein glycosylation can play a key role in these processes and has previously been shown to be a critical modulator of ion channel gating, trafficking and stability [13-16]. *N*-linked glycosylation occurs within the ER and undergoes further modifications within the GC [17]. A large, preformed oligosaccharide precursor is added to the nascent protein within the ER. Trimming of specific glycans signals that the glycoprotein is ready for transport to the GC for further processing. If the glycosylated protein is unfolded or misfolded, a glucose residue is added back to the initial oligosaccharide, preventing its export to the GC [18,19]. Correct conformation of the protein triggers removal of this glucose residue and protein release from the ER. Similarly, within the GC sugar moieties are rearranged. The final composition and glycan number regulates glycoprotein trafficking and stability [18,20]. N-glycosylation occurs on Asn in NXS/T motifs. Both $K_{2P}3.1$ and $K_{2P}9.1$ carry a conserved, predicted glycosylation site at position 53. We sought, therefore to determine whether these channels are glycosylated in vivo and if glycosylation has a regulatory role in channel

EXPERIMENTAL PROCEDURES

Molecular biology

function.

HA-(YPYDVPDYA) tagged rat (r) $K_{2P}3.1$ has been described previously [10]. Similarly, the HA tag was introduced into GFP-r $K_{2P}9.1$ between A213 and L214, using Pfu Ultra DNA polymerase (Agilent Technologies UK Ltd, Stockport, UK). A conserved, putative glycosylated asparagine, N53, was altered to glutamine in $rK_{2P}3.1$ and $rK_{2P}9.1$,

GFP-r $K_{2P}3.1$ and GFP-r $K_{2P}9.1$, and the HA-tagged GFP-r $K_{2P}3.1$ and GFP-r $K_{2P}9.1$ (Table 1), also using Pfu Ultra DNA polymerase. DNA constructs were fully sequenced before use.

Western blotting

COS-7 cells were plated at 5 x 10⁵ cells per 10 cm dish in DMEM / 10% FCS, then transiently transfected with 10 μg DNA encoding GFP- $rK_{2P}3.1$ -HA, GFP- $rK_{2P}3.1_{N53Q}HA$, GFPrK_{2P}9.1-HA or GFP-rK_{2P}9.1_{N53O}HA, using jetPEI transfection reagent, according to the supplier's instructions (Polyplus, Source **Bioscience** Autogen, Nottingham, UK). DNA-PEI complexes were removed from cells after 4 h and replaced with fresh DMEM / 10% FCS. Transfected cells were allowed to recover for 1 h, then tunicamycin (or an equivalent volume of DMSO) added to a final concentration of 1.0 µg/ml. Control and tunicamycin-treated samples were incubated for 16 h overnight at 37°C, 5% CO₂. Cells were harvested by scraping on ice, in PBS supplemented with a protease inhibitor cocktail (Thermo Fisher Scientific, Perbio Science UK, Ltd, Cramlington, UK), washed in PBS, then lysed for 30 min on ice in 200 µl lysis buffer (10 mM Tris, pH 7.5, 150 mM NaCl, 0.5% NP-40) supplemented with protease inhibitors. Lysates were centrifuged at 5000 g for 5 min at 4°C and the post-nuclear supernatant was mixed with protein sample buffer containing 100 mM DTT (final) for K_{2P}9.1 and 200 mM DTT (final) for K_{2P}3.1 and incubated for 30 min at room temperature. Samples were separated bv SDS-polyacrylamide gel electrophoresis (PAGE) and transferred nitrocellulose membranes. The membranes were probed with either 1/1000 rabbit anti-GFP antibody (for K_{2P}3.1, ab290, Abcam, Cambridge, UK) or 1/1000 dilution anti-HA tag antibody (for K_{2P}9.1, mouse clone 16B12, Covance, Leeds, UK), then a horseradish peroxidase-conjugated antirabbit or anti-mouse secondary antibody (Dako UK Ltd, Ely, UK), followed by detection using Pierce Super Signal West (Thermo Fisher Scientific).

Whole cell patch clamping recordings

HEK293 cells were plated on 22 mm sterile coverslips in 6-well plates at 10^5 cells per well. After 3 hours, cells were transiently transfected with either 1.5 µg untagged, full-length $rK_{2P}3.1$ or $rK_{2P}3.1_{N53Q}$, or 0.1 - 0.25 µg $rK_{2P}9.1$ or $rK_{2P}9.1_{N53Q}$ in pcDNA3.1 and 0.75 µg eGFP-C1 per well of a

6-well plate (Clontech, Saint-Germain-en-Laye, France), as described above. Controls were nongreen fluorescent cells in the transfection wells.

Green fluorescent cells were selected for whole cell patch clamp analysis 24 h posttransfection. Pipette solution was K+-rich and contained 150 mM KCl, 1 mM MgCl₂, 10 mM HEPES, 2 mM EGTA, pH 7.2, with KOH; free $[Ca^{2+}] = 27$ nM. Bath solution was Na⁺-rich and contained 135 mM NaCl, 5 mM KCl, 1 mM MgCl₂, 10 mM HEPES, 1 mM CaCl₂, pH 7.8, with NaOH. All experiments were carried out at temperature. Patch pipettes manufactured from standard-walled borosilicate glass capillary tubing (1B150-4, World Precision Instruments) on a two-stage Narishige PC-10 pipette puller (Narishige Scientific Instrument Laboratory, Kasuya, Tokyo, Japan), were heatpolished on a Narishige microforge, and had measured tip resistances of 2–5 $M\Omega$ (when filled with K⁺-rich pipette solution). Resistive feedback voltage-clamp was achieved using an Axopatch 200 B amplifier (Axon Instruments, Foster City, CA). Voltage protocols were generated and currents were recorded using Clampex 10.2 employing Digidata 1400A (Axon Instruments). Data were filtered (4-pole Bessel) at 1 kHz and digitized at 5 kHz. Following successful transition to the whole-cell recording mode, capacitance transients were compensated for and measured. To evoke ionic currents voltage step protocol (-100 mV to 90 mV in 10 mV increments, 100 ms) was employed and current-voltage relationships constructed from plateau stage of each 100 ms step.

Flow cytometry

COS-7 cells were plated in 10 cm dishes, 5 x 10⁵ per dish and transfected transiently with 10 µg plasmid DNA encoding GFP-rK_{2P}3.1-HA, GFP-rK_{2P}3.1_{N53Q}HA, eGFP alone or empty pcDNA3.1 (Invitrogen, Paisley, UK), as described above. In tunicamycin-treated samples, the transfected cells were allowed to recover for 1 h before addition of the antibiotic (1.0, 0.1 or 0.01 µg/ml final concentration) or DMSO alone. After overnight incubation (16 h), cells were harvested using trypsin, then stained at room temperature, with occasional gentle agitation, for 1 h with anti-HA-tag antibody (Covance) at 1/400 dilution, or an isotype control (IgG1, Invitrogen), followed by

goat anti-mouse F(ab')₂ fragment conjugated to Alexa Fluor 647 (Invitrogen; 1 h at room temperature; darkness; 1/1000 dilution). Immediately prior to analysis, cells were stained with SYTOX AADvanced Dead Cell Stain (Invitrogen) to exclude damaged cells from the subsequent flow cytometric analyses (FACSCanto, BD Biosciences, Oxford, UK). Surface expression for each sample was calculated as the mean fluorescence intensity (MFI) of HA-tag-stained cells minus the MFI of the corresponding isotype control. For low glucose experiments, COS-7 cells were grown in DMEM / 10% FCS containing 1 g/l glucose ('low') or 4.5 g/l glucose ('high') for 3 to 10 days, before transfection and analysis, as described above.

Microscopy

COS-7 cells were transfected transiently with DNA constructs encoding GFP-rK_{2P}3.1-HA, GFPrK_{2P}3.1_{N53O}HA, GFP-rK_{2P}9.1 or GFP-rK_{2P}9.1_{N53O}, on coverslips, as described above, cultured overnight, then fixed with 4% w/v formaldehyde in PBS for 7 min at RT, blocked with 3% w/v BSA in PBS and stained with anti-HA-tag antibody and goat anti-mouse F(ab')₂ fragment conjugated to Alexa Fluor 647, or with biotinylated anti-mouse (Vector Laboratories, Burlingame, CA) and streptavidin-Texas Red (Vector Laboratories) as described above. For co-localisation studies, fixed cells were permeabilised with 0.1% Triton-X-100 in PBS before the blocking step. Primary antibodies were: mouse anti-58K Golgi protein (1/1000 dilution, clone 58K-9, Abcam), rabbit anti-ERGIC-53 (1/100 dilution, Sigma) and goat anti-EEA1 (1/100 dilution, C-15, Santa Cruz).

For the recycling assay, COS-7 cells were transfected transiently with GFP-rK_{2P}3.1-HA or GFP-rK_{2P}3.1_{N53O}HA, cultured overnight, then incubated for 2 h in DMEM without FCS. After 90 min, cycloheximide (Sigma) was added to a final concentration of 100 µg/ml. At 2 h, the cells were moved to a cold room (4 °C), placed on ice for 45 min, then washed three times in ice-cold PBS. Surface proteins were biotinylated for 45 min on ice using 0.5 mg EZ-Link NHS-SS-Biotin, (Thermo Fisher Scientific) per well of a 6-well plate. Cells were then returned to DMEM / 10% FCS / 100 µg/ml cycloheximide and incubated for 0 and 20 min. At each time point, coverslips were transferred to wells containing ice-cold biotin stripping buffer (50 mM sodium methanethiolate, 50 mM Tris-HCl pH 8.6, 100 mM NaCl, 1 mM MgCl₂, 0.1 mM CaCl₂), where they were incubated on ice for 15 min, the buffer exchanged and then the incubation repeated. The stripping step was to remove non-internalised biotin from the plasma membrane. Coverslips were then rinsed with ice-cold PBS, fixed with formaldehyde as described above and stained for EEA1 and biotin. Biotin was detected with a streptavidin-Alexa Fluor 546 conjugate (Invitrogen). Triple-stained vesicles were identified by drawing transects through regions of interest and looking for areas of signal overlap in all three dimensions. Quantitative analysis was carried out using Imaris 7.5.2 software.

Coverslips were mounted and visualised using either a Zeiss Axio Observer D1 or using a Leica TCS SP5 confocal scanning microscope in the University of Southampton Biomedical Imaging Unit.

Statistics

Graph and statistical analysis software SigmaPlot 11.0 (Systat Software, Chicago, IL) was used to plot electrophysiology data and perform significance tests. Data were first subjected to the Shapiro-Wilk test for normality. Normal populations were analysed using Student's *t*-test. Non-normal populations were analysed using the Mann-Whitney rank sum test.

RESULTS

Glycosylation of K_{2P} channels

Protein sequences of human, mouse and rat K_{2P} channels were analysed for the presence of *N*-glycosylation consensus sites using the NetNGlyc 1.0 server [21] (http://www.cbs.dtu.dk/services/NetNGlyc). Sites with a glycosylation potential ≥ 0.5 were crosschecked for predicted external domains. Thirteen of the fifteen mammalian K_{2P} channels sequenced to date contain at least one predicted glycosylation site within at least one of the three species examined (Table 2). Notably, using a threshold glycosylation potential ≥ 0.5 , neither $K_{2P}1.1$ (TWIK) nor K_{2P}15.1 were predicted to be glycosylated. However, K_{2P}1.1 does contain a glycosylation consensus sequence at positions 95-97 (conserved between human and rodent) with N95 as a potential glycan acceptor. Lesage et al. (1996) reported K_{2P}1.1 to be a glycoprotein, due to altered band sizes following separation by PAGE

of glycopeptidase treated channels [22]. Significantly, $K_{2P}15.1$, which to date has failed to show functional expression, is the only K_{2P} channel that lacks an N-glycosylation consensus site (Table 2).

Both $K_{2P}3.1$ and $K_{2P}9.1$ possess a single N-glycosylation site at position 53 (N53; $rK_{2P}3.1$ position potential = 0.689; $rK_{2P}9.1$ = 0.802). N53 is located within the first external domain adjacent to the first pore and is conserved within all species examined (Fig. 1A and B).

To determine whether N53 is in fact a target for glycan attachment, we abolished the predicted glycosylation site by substitution of glutamine for asparagine, creating the mutant GFP-rK_{2P}3.1_{N53O}HA channels and rK_{2P}9.1_{N53O}HA. We examined whether the wildtype and glycosylation mutant channels were glycosylated when expressed in COS-7 cells. COS-7 cells transiently expressing GFP-rK_{2P}3.1-HA, GFP-rK_{2P}3.1_{N53O}HA, GFP-rK_{2P}9.1-HA and GFP-rK_{2P}9.1_{N530}HA were either treated with 1.0 µg/ml tunicamycin, which blocks synthesis of all N-glycans, or its vehicle DMSO alone. The relative mobility of the tagged channels from total cell lysates was compared by SDS-PAGE, followed by Western blotting. For K_{2P}3.1, two distinct bands are detected in the non-treated wildtype lane; on treatment with tunicamycin or in cells transfected with GFP-rK_{2P}3.1_{N530}HA, the intensity of the upper band is decreased, while that of the lower band increases, suggesting a higher proportion of higher mobility channels (Fig. 1C). Untreated, wild-type K_{2P}9.1 channels migrate as a single band to the predicted weight. A proportion of K_{2P}9.1 from the tunicamycin-treated cells migrated further than their untreated controls, while glycosylation mutant channels show mobility similar to the tunicamycin-treated wildtype channel and higher than the glycosylated wild-type channel (Fig. 1C).

Disruption of $K_{2P}3.1$ glycosylation prevents channel functional expression.

To determine if channel glycosylation impacts channel function, we investigated the electrophysiological properties of wild-type and N53Q mutant $rK_{2P}3.1$ in HEK293 cells. Cells expressing wild-type channel show a current-voltage (I-V) relationship typical of K_{2P} potassium leak channels, with a reversal potential of

 $-60.88 \text{ mV} \pm 3.20$, (n=8; Fig. 2A). As predicted for TASK family members, rK_{2P}3.1 currents were inhibited by exposure to acidic external solutions (pH 6.5) with currents at 60 mV reduced from 0.97 ± 0.17 nA at pH 7.8 to 0.45 ± 0.08 nA at pH 6.5 which is not significantly different from currents produced by untransfected cells (0.39±0.09 nA at pH 7.8 n=8); p=0.63; Fig. 2A and B). HEK293 cells transiently expressing rK_{2P}3.1_{N53O} channels failed to produce current significantly different from untransfected cells at both pH 7.8 and pH 6.5 $(0.41\pm0.08 \text{ nA} \text{ at pH} 7.8, n=7), p=0.81;$ 0.43±0.10 nA at pH 6.5 n=9), p=0.79 (Fig. 2A and B). This decrease in rK_{2P}3.1_{N53Q} current compared to wild-type rK_{2P}3.1 current is coupled with a more positive reversal potential, (-31.22± 6.01 mV) which is predicted if background K⁺ flux is reduced.

To determine whether the observed decreased flux is due to altered channel function or a reduced number of channels on the cell surface, channel cellular localisation and expression on the cell surface was investigated in COS-7 cells transiently expressing either the wild-type or glycosylation mutant K_{2P}3.1 channels. Channel constructs contained an internal N-terminal GFP tag plus a non-interfering HA tag incorporated into an external loop within the second pore-forming domain of the channel. The GFP-tag made it possible to monitor total expression (internal and cell surface) of the wild-type and mutant channel. The external HA-tag enabled quantitative comparison of the relative amount of each channel expressed at the cell surface by means of staining non-permeablised cells with anti-HA antibodies, followed by flow cytometry (Fig. 2C and D).

In a typical experiment, the mean surface expression level of double-tagged $rK_{2P}3.1_{N53Q}$ in live, intact cells was only 9% relative to the wild-type channel, as measured by staining externally with anti-HA-tag (Fig. 2C MFI values as follows: GFP-rK_{2P}3.1-HA, 294; GFP-rK_{2P}3.1_{N53Q}HA, 97; isotype control, 78). Significantly, when cells expressing double-tagged $rK_{2P}3.1$ channels were treated with 1.0 μ g/ml tunicamycin, a reduction in HA-tag fluorescence was observed (MFI 101), comparable to cells expressing the mutant channel. Over a series of experiments, summarised in Fig. 2D, disruption of glycosylation by mutation of the channel always resulted in very low cell surface expression of $K_{2P}3.1_{N53Q}$ (mean 11.3% relative to

wild-type $K_{2P}3.1$; SEM 1.1%, n=4). Chemical inhibition of glycosylation by tunicamycin resulted in an average surface expression of 19.8% relative to wild-type $K_{2P}3.1$ (SEM 4.6%, n=3).

Images from immunofluorescence experiments comparing cellular localisation of tunicamycin-treated and non-treated wild-type rK_{2P}3.1 channels together with mutant channels supported the flow cytometry data. When wildtype channels bearing both GFP and external HA tag (GFP-rK_{2P}3.1-HA) were transiently expressed in COS-7 cells, total channel protein expression was detected by GFP fluorescence (Fig. 2E, upper 'Merge' panels: green), while cell surface channel was detected using anti-HA-tag antibody (red). GFP fluorescence is visible in all four samples: untreated and tunicamycin-treated cells expressing wild-type and N53Q mutant K_{2P}3.1. Anti-HAstaining, however, was only detected on the surface of untreated cells expressing wild-type channel (Fig. 2E, lower panels). Taken together these data support the conclusion that disruption of channel glycosylation has a negative effect on cell surface expression of $rK_{2P}3.1$.

External glucose concentration has been reported to impact protein glycosylation [23]. We wanted to test if reducing external glucose concentration might modulate the surface expression of rK_{2P}3.1. Cells transiently expressing GFP-rK_{2P}3.1-HA were cultured under normal cell culture glucose concentrations (4.5 g/l or 25 mM) and reduced glucose (1.0 g/l or 5.6 mM), then flow cytometry (Fig. 3A) and confocal microscopy (Fig. 3B) used to probe cell surface expression, detected by anti-HA staining. Both methods demonstrate a modest but consistent reduction in channel cell surface expression. In a typical flow cytometry experiment (Fig. 3A), cell surface HA-tag fluorescence in cells cultured in low external glucose was 84% relative to control glucose concentrations (4.5 g/l); over six experiments, the mean value was $88.2 \pm 3.8\%$ of the control. This reduced cell surface expression in response to reduced external glucose was not detected for the glycosylation mutant channel rK_{2P}3.1_{N53Q} (Fig. 3). These data suggest that $K_{2P}3.1$ cell surface expression is linked to glucose concentration.

 $K_{2P}9.1$ cell surface expression is less sensitive to channel glycosylation state.

The impact of disrupting rK_{2P}9.1 glycosylation was investigated by examining the functional expression of both the wild-type and glycosylation mutant rK_{2P}9.1 channels by patch clamp analysis, together with examining cell surface expression of the channels by flow cytometry immunofluorescence. evoked Currents from HEK293 cells transiently expressing either wildtype or glycosylation mutant channels showed no significant difference in channel kinetics, current amplitude or reversal potential (Fig. 4A and B). Reversal potential of HEK293 cells expressing $rK_{2P}9.1 \text{ was } -67.23 \pm 1.31 \text{ mV (n=13)}$ compared to $-60.00 \pm 5.78 \text{ mV (n=9)}$ for rK_{2P}9.1_{N53O}. At 60 mV test potential maximum current at pH 7.8 for wildtype channels was $2.36 \pm 0.47 \, \text{nA}$ compared to 2.91 ± 0.56 nA for mutant channels (p=0.46).

The mean surface expression level of GFP- and HA-tagged rK_{2P}9.1_{N53O} from three independent experiments was 63.6%, SEM 1.7, relative to the wild-type channel, when measured by flow cytometry (Fig. 4C MFI values as follows: GFP-rK_{2P}9.1-HA, 433; isotype control, 53; GFP $rK_{2P}9.1_{N530}HA$, 287; isotype control, Although there was a clear difference in MFI, there was considerable overlap between the range of fluorescence intensities of cells expressing wild-N530 mutant channels. type and Immunofluorescence microscopy (Fig. 4D) also indicated a reduction in the amount of cell surfacelocalised GFP-rK_{2P}9.1_{N530}HA, compared to wildtype channel, but this reduction was less marked in comparison to GFP-rK_{2P}3.1_{N53O}HA (Fig. 2E).

Cellular localisation of wild-type and glycosylation mutant channels.

As the non-glycosylated rK_{2P}3.1_{N53O} channel shows marked reduction in cell surface expression compared to the wild-type channel and nonglycosylated proteins are often retarded through the secretory pathway, we asked whether the glycosylation mutant channel experienced altered trafficking to the cell surface. Previous studies have reported an ER distribution for TASK channels [7, 24]. We consistently observe a $K_{2P}3.1$ and K_{2P}9.1 perinuclear accumulation in transfected cells, as well as a generalised ER staining pattern, which co-localises with an ER resident, protein disulphide isomerase. The perinuclear staining was more frequent and pronounced in the N53Q channel mutants. To characterise the subcellular

localisation of both the wild-type glycosylation mutant K_{2P}3.1 we used markers for ERGIC (ERGIC-53) and GC (58K Golgi protein). COS-7 cells transiently expressing either GFPrK_{2P}3.1 or GFP-rK_{2P}3.1_{N53O} showed overlap between channel signal and each of the compartments examined (Fig. 5). To determine if signal from the GFP-tagged channel localised specifically with signal for each of the subcellular compartments examined, the intensity of both signals (channel: green and compartment: red) were quantified and compared along defined transects. This analysis revealed partial overlap with the 58K Golgi protein for both wild-type and mutant channels (Fig. 5A), while substantial signal overlap was observed for both channels with ERGIC-53 (Fig. 5B). Comparable experiments were performed for rK_{2P}9.1 and rK_{2P}9.1_{N53O} with results (Supplemental Fig. Significantly, both the wild-type and glycosylation mutants for both channels were observed beyond the ER and detected in both the ERGIC and GC compartments, providing evidence that the lack of channel glycosylation does not completely block forward transport of these channels.

Does channel stability contribute to reduced function of glycosylation mutant $rK_{2P}3.1_{N530}$?

The total expression (both intracellular and cell surface) of GFP-tagged wild-type rK_{2P}3.1 could be compared with the GFP-tagged N53Q mutant channel by quantitation of GFP fluorescence. In six flow cytometry experiments, the GFP-rK_{2P}3.1_{N53O}-HA expression of reproducibly lower than the wild-type channel. In a typical experiment (Fig. 6A), the MFI (GFP fluorescence) of cells expressing GFP-rK_{2P}3.1-HA was 24900, while that of GFP-rK_{2P}3.1_{N53Q}HA was 17740. Tunicamycin-treatment reduced the MFI of cells expressing wild-type channel to 18400, compared to 16460 for the N53Q mutant. We reasoned that lower total amounts of nonglycosylated channel may arise due to enhanced turnover, whether the mutant channel is targeted for degradation direct from the ER, and/or is very rapidly retrieved from the plasma membrane, given that rK_{2P}3.1_{N53O} is not detected at the cell surface but does proceed through the secretory system.

Adopting a sensitive plasma membrane biotinylation method [25] we tested whether non-

glycosylated rK_{2P}3.1 could be detected in newly formed endocytic vesicles. COS-7 cells expressing GFP-rK_{2P}3.1 (Fig. 6B, WT panel) or GFPrK_{2P}3.1_{N53O} (Fig. 6C, N53Q panel) underwent cell surface biotinvlation followed by a period of endocytic endocytosis. Numerous containing biotin were visible after a 20 min incubation of surface-labeled transfected cells (Fig. 6B and C, Biotin panels). Many of the vesicles containing biotinylated cell surface material also stained positive for the early endosome marker, Early Endosome Antigen 1 (EEA1; Fig. 6B and C, EEA1 panels). A further subset of these vesicles was triple-stained, containing GFP-tagged wild-type or N53Q mutant channel, biotin and EEA1 (Fig. 6B and C, Merge panels). The number of triple-stained vesicles for each channel was quantified, in cells transfected with wild-type $K_{2P}3.167 \pm 18$ (n=4 fields of view) triple stained vesicles were identified. A similar number (77 \pm 19; n=7) of triple-stained vesicles were identified in cells transfected with the glycosylation mutant channel. Four example transects for GFP-rK_{2P}3.1 and GFP-rK_{2P}3.1_{N530} illustrate co-localisation of channel, biotin and in individual triple-stained vesicles EEA1 (numbered 1 - 4 in Fig. 6A and B, Merge panels). These results indicate that rK_{2P}3.1_{N53O} does reach the plasma membrane and like wild-type $rK_{2P}3.1$ is retrieved in endocytic vesicles.

DISCUSSION

Glycosylation of membrane proteins is a common post-translational modification with a variable role in the processing and function of glycoproteins [26]. In this study we examined the prospect and impact of N-glycosylation on members of the K_{2P} family of background potassium channels with particular focus on TASK channels (K_{2P}3.1 and $K_{2P}9.1$) and demonstrate a conserved N-linked glycosylation site at N53. Although membrane proteins may possess an N-glycosylation consensus sequence, it is worth noting that not all predicted sites undergo glycan modification. This was recently demonstrated for K_{2P}18.1 (or TRESK), when two sites were predicted to undergo N-linked glycosylation but only one was shown to accept glycans [27]. The best estimate for the proportion of all proteins glycosylated has been revised substantially downwards from over

50% to under 20% [28] underlining the importance of experimentally verifying predicted glycosylation sites. Therefore, TASK channel glycosylation was verified by electrophoresis mobility shift assays and revealed that prevention of acceptance of glycosylation alters the molecular weight and hence mobility of these channels.

Channel glycosylation was shown to be critical for cell surface expression and hence function of K_{2P}3.1. Patch clamp analysis, flow cytometry and immunofluorescence studies all verify that K_{2P}3.1_{N53O} targeting to the cell surface disrupted. Similarly, cells transiently expressing wild-type channels treated with (which tunicamycin inhibits N-linked glycosylation) showed cell surface expression comparable to cells expressing the glycosylation mutant channels (K_{2P}3.1_{N53O}), supporting a regulatory role for channel glycosylation in K_{2P}3.1 surface expression and validating that the altered surface expression is due to removal of the glycan tree rather than substitution of the Asn. Furthermore, when cells expressing wild-type K_{2P}3.1 were cultured in glucose concentrations lower than standard cell culture conditions, a 12% reduction in cell surface expression of K_{2P}3.1 was detected by flow cytometry, with reduced surface expression of the channel detected immunofluorescence. Together, these data provide evidence that K_{2P}3.1 surface expression and function are sensitive to the glycosylation state of the channel.

Channel glycosylation has less impact on the surface expression and function of $K_{2P}9.1$. K_{2P}9.1_{N53O} displayed a circa 40% reduction in mean surface expression when compared to the wild-type channel and quantified by flow cytometry. Channel current for wild-type and glycosylation mutant K_{2P}9.1 channels were not significantly different when analysed by patch clamp analyses. These data support the conclusion that while K_{2P}9.1 is clearly glycosylated at N53, lack of glycosylation at this site is not critical to the channel's surface expression and delivery and does not significantly affect channel function but has a negative impact on the overall level of channel maintained on the cell surface either by altering the efficiency of channel delivery to, or removal from the cell surface.

Such varied response of two closely-related ion channels to glycosylation is not

unprecedented. Indeed. members of hyperpolarization-activated cyclic nucleotidegated (HCN) channels show similar findings. HCN1 and HCN2 are both glycosylated in embryonic mouse heart [29], but whereas the surface expression of HCN2 is highly dependent on glycosylation, HCN1 is markedly less sensitive. The authors propose that the channels diverged after gene duplication from an ancestor HCN channel that did not require glycosylation for efficient cell surface localisation.

The recently solved crystal structures of two K_{2P} channels: $K_{2P}1.1$ and $K_{2P}4.1$ [30, 31] were obtained using recombinant proteins from which putative glycosylation sites had been removed. The respective predicted glycosylation sites occur within a disordered region after the extracellular cap/helical cap domain and appear to be positioned away from the ion selectivity filter in each channel. We can postulate a similar arrangement for N53 in $K_{2P}3.1$ and $K_{2P}9.1$, which likely places the *N*-glycan away from the channel pore and selectivity filter: in support of this, the biophysical properties of $K_{2P}9.1_{N53Q}$ did not appear to be altered when examined by whole-cell patch clamp recordings.

Among their other roles, glycans have been proposed to act as targeting determinants for a number of channels, including aquaporins (AQP-2), voltage-gated potassium channels (Kv1.2), HCN channels and acid-sensing ion channels (ASIC-1a) [29, 32-34]. It is difficult, however, to discriminate between sorting per se and the protein quality control processes that precede targeting. The β-subunit of gastric HK-ATPase is an example of a protein where N-linked glycans have been shown to play a distinct role in targeting to the apical plasma membrane [35]. The almost complete absence of $K_{2P}3.1_{N53O}$ on the plasma membrane led us to investigate whether intracellular localisation of the glycosylation mutant channel was disrupted.

When the intracellular localisation of wild-type $K_{2P}3.1$ and mutant $K_{2P}3.1_{N53Q}$ were compared by immunofluorescence, both channels were detected in both the ERGIC and the GC. Indeed, while a degree of overlap between the GC marker and the channel was detected, substantially greater overlap between ERGIC marker and both channels was observed. Significantly, ERGIC contributes to the concentration, folding and

quality control of newly synthesised proteins. These findings are significant as they suggest that although the non-glycosylated channel is not detected on the cell surface, it does escape the ER and trafficks to the ERGIC and GC. Therefore it appears that glycosylation does not in itself alter the processing pathway of $K_{2P}3.1$ channels.

If glycosylation mutant channels are not retained within the ER and pass through the secretory pathway, these channels have the possibility of two fates. Mutant channels may reach the cell surface, but show lower stability and hence higher rate of turnover, or they may be targeted directly for degradation. As N-linked glycosylation of K_{2P}3.1 channels does not appear to alter intracellular transport of the channel, we sought to determine whether glycosylation had an impact on channel turnover. By flow cytometry, a reduction in the total (intracellular and cell surface) amount of K_{2P}3.1_{N53O} per cell, compared to the wild-type was observed. Similarly, tunicamycin-treated cells expressing $K_{2P}3.1$ showed a similar reduction, with total channel per cell comparable to ablation of the glycosylation site. These observations are significant when considered together with our recycling data. When channel retrieval from the cell surface and entry into the endocytic pathway is studied, although K_{2P}3.1_{N53O} is not detected on the cell surface, K_{2P}3.1_{N53O} which was tagged by surface labelling with biotin (and therefore must have reached the cell surface) is detected within the endocytic pathway. Together these data suggest that although K_{2P}3.1 cannot be detected at the cell surface, a proportion of the channel population does reach the plasma membrane but is retrieved and likely targeted for degradation via the endocytic pathway. These studies provide strong evidence that channel glycosylation plays an important role in the stability of $K_{2P}3.1$ expression on the cell surface.

How might glycosylation contribute to the stability of $K_{2P}3.1$ once delivered to the plasma membrane? The two glycans on wild-type CFTR have been shown to promote proper apical recycling; in their absence, CFTR is more rapidly internalised and is targeted to the basolateral membrane, where it appears to have a shorter half-life than glycosylated CFTR [36]. The same glycans also play a role in the stability of the channel once it

has exited the ER [36]. A subset of the N-glycans attached to the HK-ATPase β is responsible for delivery of the protein to the apical membrane and retaining it there [35]. It has been suggested that extracellular lectins may play a role in binding HK-ATPase and stabilising it at the cell surface [37]. Glycosylation increases thermodynamic stability by reducing the amount of surface area accessible to solvent, which in turn influences structural dynamics and protein function [26]; this effect has been clearly demonstrated for the thermostability of human aquaporin 10 protein [39]. While a number of potential mechanisms exist, it will be important to find out how glycosylation contributes to the stability of K_{2P}3.1 and to determine the process that renders $K_{2P}9.1$ less sensitive to this regulation.

TASK channels are expressed in both neuronal and cardiac cell populations and significantly have been identified in glucosesensing neurons of the hypothalamus, as well as peripheral specialised chemo- and nutrient-sensing

cells [40, 41]. Sensitivity of $K_{2P}3.1$ cell surface expression and turnover to its glycosylation state represents a potential link between metabolic status and cellular activity. Down-regulation of TASK channels is known to influence cellular depolarisation. Hence, decreased cell surface expression of $K_{2P}3.1$ channels in response to decreased glucose would lead to increased neuronal excitation. Furthermore, in the diabetic patient, with sustained higher blood glucose levels, one would predict that this environment would promote $K_{2P}3.1$ channel surface expression with resultant dampening of cellular activity.

The importance of the findings presented in this study lies in the numerous roles TASK channels may play in cellular regulation. Their varied sensitivity and stability to glycosylation, and by association glucose concentration, opens a host of potential regulatory pathways in which these important channels may be involved.

REFERENCES

- 1. Goldstein, S.A., Bockenhauer, D., O'Kelly, I., and Zilberberg, N. (2001) Potassium leak channels and the KCNK family of two-P-domain subunits. *Nat. Rev. Neurosci.* **2**, 175-184
- 2. Lotshaw, D.P. (2007) Biophysical, pharmacological, and functional characteristics of cloned and native mammalian two-pore domain K⁺ channels. *Cell Biochem. Biophys.* **47**, 209-256
- 3. Enyedi, P. and Czirják, G. (2010) Molecular background of leak K⁺ currents: two-pore domain potassium channels. *Physiol. Rev.* **90**, 559-605
- 4. Buckler, K. J., Williams, B. A., and Honoré, E. (2000) An oxygen-, acid- and anaesthetic-sensitive TASK-like background potassium channel in rat arterial chemoreceptor cells. *J. Physiol.* **525**, 135-142
- 5. Patel, A. J., Honoré, E., Lesage, F., Fink, M., Romey, G., and Lazdunski, M. (1999) Inhalational anesthetics activate two-pore-domain background K⁺ channels. *Nat. Neurosci.* **2**, 422-426
- 6. Sirois, J. E., Lei, Q., Talley, E. M., Lynch, C. 3rd, and Bayliss, D. A. (2000) The TASK-1 two-pore domain K^+ channel is a molecular substrate for neuronal effects of inhalation anesthetics. *J. Neurosci.* **20**, 6347-6354
- 7. O'Kelly, I., Butler, M. H., Zilberberg, N., and Goldstein, S. A. (2002) Forward transport. 14-3-3 binding overcomes retention in endoplasmic reticulum by dibasic signals. *Cell* **111**, 577-588

- 8. Rajan, S., Preisig-Muller, R., Wischmeyer, E., Nehring, R., Hanley, P. J., Renigunta, V., Musset, B., Schlichtorl, G., Derst, C., Karschin, A., and Daut, J. (2002) Interaction with 14-3-3 proteins promotes functional expression of the potassium channels TASK-1 and TASK-3. *J. Physiol.* **545**, 13-26
- 9. O'Kelly, I. and Goldstein, S.A.N. (2008) Forward transport of $K_{2P}3.1$: mediation by 14-3-3 and COPI, modulation by p11. *Traffic* **9**, 72-78
- 10. Mant, A., Elliott, D., Eyers, P.A., and O'Kelly, I.M. (2011) Protein kinase A is central for forward transport of two-pore domain potassium channels K_{2P}3.1 and K_{2P}9.1. *J. Biol. Chem.* **286**, 14110-14119
- 11. Delisle, B., Anson, B., Rajamani, S., and January, C. (2004) Biology of cardiac arrhythmias: ion channel protein trafficking. *Circ. Res.***94**, 1418-1428
- 12. Mathie, A., Rees, K.A., El Hachmane, M.F., and Veale, E.L. (2010) Trafficking of neuronal two pore domain potassium channels. *Curr. Neuropharmacol.* **8,** 276-286
- 13. Gong, Q., Anderson, C.L., January, C.T., and Zhou, Z. (2002) Role of glycosylation in cell surface expression and stability of HERG potassium channels. *Am. J. Physiol. Heart Circ. Physiol.* **283**, 77-84
- 14. Helenius, A., and Aebi, M. (2004) Roles of N-linked glycans in the endoplasmic reticulum. *Annu. Rev. Biochem.* **73**, 1019-1049
- 15. Cohen, D.M. (2006) Regulation of TRP channels by N-linked glycosylation. *Semin. Cell Dev. Biol.* **17**, 630-637
- 16. Hall, M.K., Cartwright, T.A., Fleming, C.M., and Schwalbe, R.A. (2011) Importance of glycosylation on function of a potassium channel in neuroblastoma cells. *PLoS One.* **6**, e19317
- 17. Schwarz, F. and Aebi, M. (2011) Mechanisms and principles of N-linked protein glycosylation. *Curr. Opin. Structural Biol.* **21**, 576-582
- 18. Aebi, M., Bernasconi, R., Clerc, S., and Molinari, M. (2010) N-glycan structures: recognition and processing in the ER. *Trends Biochem. Sci.* **35**, 74-82
- 19. Appenzeller-Herzog, C. and Hauri, H.P. (2006) The ER-Golgi intermediate compartment (ERGIC): in search of its identity and function. *J. Cell Sci.* **119**, 2173-2183
- 20. Kamiya, Y., Satoh, T., and Kato, K. (2012) Molecular and structural basis for N-glycan-dependent determination of glycoprotein fates in cells. *Biochim. Biophys. Acta.* **1820**, 1327-1337
- 21. Blom, N., Sicheritz-Pontén, T., Gupta, R., Gammeltoft, S., and Brunak, S. (2004) Prediction of post-translational glycosylation and phosphorylation of proteins from the amino acid sequence. *Proteomics* **4**, 1633-1649
- 22. Lesage, F., Guillemare, E., Fink, M., Duprat, F., Lazdunski, M., Romey, G., and Barhanin, J. (1996) TWIK-1, a ubiquitous human weakly inward rectifying K⁺ channel with a novel structure. *EMBO J.* **15**, 1004-1011

- 23. Hayter, P.M., Curling, E.M., Baines, A.J., Jenkins, N., Salmon, I., Strange, P.G., Tong, J.M., and Bull, A.T. (1992) Glucose-limited chemostat culture of Chinese hamster ovary cells producing recombinant human interferon-gamma. *Biotechnol. Bioeng.* **39**, 327-335
- 24. Renigunta, V., Yuan, H., Zuzarte, M., Rinné, S., Koch, A., Wischmeyer, E., Schlichthörl, G., Gao, Y., Karschin, A., Jacob, R., Schwappach, B., Daut, J., and Preisig-Müller, R. (2006) The retention factor p11 confers an endoplasmic reticulum-localization signal to the potassium channel TASK-1. *Traffic* 7, 168-181
- 25. Richardson, D. S. and Mulligan, L. M. (2010) Direct visualization of vesicle maturation and plasma membrane protein trafficking. *J. Fluoresc.* **20**, 401-405
- 26. Sola, R. J., Rodríguez-Martínez, A., and Griebnow, K. (2007) Modulation of protein biophysical properties by chemical glycosylation: biochemical insights and biomedical implications. *Cell Mol. Life Sci.* **64**, 2133-2152
- 27. Egenberger B., Polleichtner G., Wischmeyer E., and Döring F. (2010) N-linked glycosylation determines cell surface expression of two-pore-domain K⁺ channel TRESK. *Biochem Biophys Res Commun.* **391**, 1262-1267
- 28. Khoury G.A., Baliban R.C., and Floudas C.A. (2010) Proteome-wide post-translational modification statistics: frequency analysis and curation of the swiss-prot database. *Sci. Rep.* **1**, 90
- 29. Hegle, A. P., Nazzari, H., Roth, A., Angoli, D., and Accilli, E. A. (2010) Evolutionary emergence of N-glycosylation as a variable promoter of HCN channel surface expression. *Am. J. Physiol. Cell Physiol.* **298**, C1066-C1076
- 30. Miller, A. N. and Long, S. B. (2012) Crystal structure of the human two-pore domain potassium channel K2P1. *Science* **335**, 432-436
- 31. Brohawn, S. G., del Mármol, J., and MacKinnon, R. (2012) Crystal structure of the human K2P TRAAK, a lipid- and mechano-sensitive K⁺ ion channel. *Science* **335**, 436-441
- 32. Zhu, J., Recio-Pinto, E., Hartwig, T., Sellers, W., Yan, J., and Thornhill, W.B. (2009) The Kv1.2 potassium channel: the position of an N-glycan on the extracellular linkers affects its protein expression and function. *Brain Res.* **1251**, 16-29
- 33. Moeller, H. B., Olesen, E. T. B., and Fenton, R. A. (2011) Regulation of the water channel aquaporin-2 by posttranslational modification. *Am. J. Physiol. Renal Physiol.* **300**, F1062-F1073
- 34. Jing, L., Chu, X.P., Jiang, Y.Q., Collier, D. M., Wang, B., Jiang, Q., Snyder, P. M., and Zha, X.-M. (2012) N-glycosylation of acid-sensing ion channel 1a regulates its trafficking and acidosis-induced spine remodeling. *J. Neurosci.* **32**, 4080-4091
- 35. Vagin, O., Turdikulova, S., and Sachs, G. (2004) The H,K-ATPase beta subunit as a model to study the role of N-glycosylation in membrane trafficking and apical sorting. *J Biol Chem.* **279**, 39026-39034

- 36. Cholon, D. M., O'Neal, W. K., Randell, S. H., Riordan, J. R., and Gentzsch, M. (2009) Modulation of endocytic trafficking and apical stability of CFTR in primary human airway epithelial cultures. *Am. J. Physiol. Lung Cell. Mol. Physiol.* **298**, L304-L314
- 37. Chang, X., Mengos, A., Hou, Y., Cui, L., Jensen, T. J., Aleksandrov, A., Riordan, J. R., and Gentzsch, M. (2008) Role of N-linked oligosaccharides in the biosynthetic processing of the cystic fibrosis membrane conductance regulator. *J. Cell Sci.* **121**, 2814-2823
- 38. Vagin, O., Kraut, J. A. and Sachs, G. (2009) Role of N-glycosylation in trafficking of apical membrane proteins in epithelia. *Am. J. Physiol. Renal Physiol.* **296**, F459-F469
- 39. Öberg, F., Sjöhamn, J., Fischer, G., Moberg, A., Pedersen, A., Neutze, R. and Hedfalk, K. (2011) Glycosylation increases the thermostability of human aquaporin 10 protein. *J. Biol. Chem.* **286**, 31915-31923
- 40. Duprat, F., Lauritzen, I., Patel, A., and Honoré, E. (2007) The TASK background K_{2P} channels: chemo- and nutrient sensors. *Trends Neurosci.* **30**, 573-580
- 41. O'Kelly, I., Stephens, R.H., Peers, C. and Kemp, P.J. (1999) Potential identification of the O_2 -sensitive K^+ current in a human neuroepithelial body-derived cell line. Am J Physiol. **276**, L96-L104

Acknowledgements:

This work was supported by BBSRC grant number BB/J008168/1 to Dr O'Kelly. SW and LR are funded by The Gerald Kerkut Charitable Trust. We are grateful to Dr David Johnston of the University of Southampton Biomedical Imaging Unit for assistance with confocal microscopy, Kelly Wilkinson for expert technical support and to Professor Stephen High at the University of Manchester for helpful comments.

FIGURE LEGENDS

Figure 1

 $K_{2P}3.1$ and $K_{2P}9.1$ are glycoproteins

A: Partial amino acid sequence alignment of mouse, rat and human $K_{2P}3.1$ and $K_{2P}9.1$ with *N*-linked glycosylation consensus site and channel pore selectivity sequence highlighted. **B**: Schematic membrane topology of TASK channels subunit with four transmembrane domains (dark grey), pore-forming domains (grey) and external domains (light grey) with location of putative *N*-glycosylation site depicted (N). **C**: Immunoblot showing differences in mobility of wild-type (WT) and glycosylation mutant (N53Q) TASK channels with or without prior treatment with tunicamycin to prevent the addition of *N*-linked glycans. Post-nuclear supernatants from untreated (-) or tunicamycin-treated (+) COS-7 cells transfected with GFP- and HA-tagged $K_{2P}3.1$ (upper panel) and $K_{2P}9.1$ (lower panel) were separated by SDS-PAGE and transferred to nitrocellulose. Membranes were probed with anti-GFP antibody ($K_{2P}3.1$) or anti-HA tag antibody ($K_{2P}9.1$). The positions of size standards are indicated on the left. Dotted lines indicate the middle of each band.

Figure 2

Disruption of $rK_{2P}3.1$ glycosylation prevents channel expression.

A: Electrophysiological properties of HEK293 cells transiently expressing $rK_{2P}3.1$ or $rK_{2P}3.1_{N530}$, and eGFP on separate plasmids. Traces are derived from at least 7 cells. ● Wild-type rK_{2P}3.1, external pH 7.8; o wild-type rK_{2P}3.1, external pH 6.5; \blacktriangledown rK_{2P}3.1_{N53O}, external pH 7.8; \triangle rK_{2P}3.1_{N53O}, external pH 6.5; \blacksquare untransfected cells, pH 7.8. B: Comparison of the currents from panel A at 60 mV. C: Representative flow cytometric analysis of intact COS-7 cells expressing GFP-rK_{2P}3.1-HA or GFP-rK_{2P}3.1_{N53O}-HA. Cells were stained with either a monoclonal antibody against the external HA-tag, or an isotype control antibody, followed by goat anti-mouse F(ab')₂ fragment conjugated to Alexa Fluor 647. Solid grey curve: cells expressing GFP-rK_{2P}3.1-HA, stained with the isotype control; black solid line: cells expressing GFPrK_{2P}3.1-HA and stained with anti-HA; black dashed line: cells expressing GFP-rK_{2P}3.1-HA, stained with anti-HA and treated with 1 µg/ml tunicamycin; grey solid line: cells expressing GFP-rK_{2P}3.1_{N53O}HA and stained with anti-HA; grey dashed line: cells expressing GFP-rK_{2P}3.1_{N530}HA, stained with anti-HA and treated with 1 µg/ml tunicamycin. **D**: Comparison of the surface expression of GFP-rK_{2P}3.1-HA and GFPrK_{2P}3.1_{N53O}HA +/- tunicamycin treatment, from a several flow cytometric experiments. Values are % relative to wild-type channel in untreated cells. E: Immunofluorescence images of fixed, nonpermeabilised COS-7 cells expressing GFP-rK_{2P}3.1-HA (WT) or GFP-rK_{2P}3.1_{N530}HA (N53Q), +/tunicamycin treatment. Upper panels: merged GFP (green) and anti-HA tag-conjugated fluorescence (red). Lower panels: anti-HA tag fluorescence alone. Scale bar represents 10 µm.

Figure 3 Surface expression of $rK_{2P}3.1$ responds to a reduction in the concentration of glucose in the culture medium.

A: Flow cytometric analysis of intact COS-7 cells expressing GFP-rK_{2P}3.1-HA or GFP-rK_{2P}3.1_{N53Q}HA. Cells were stained with either a monoclonal antibody against the external HA-tag, or an isotype control antibody, followed by goat anti-mouse F(ab')₂ fragment conjugated to Alexa Fluor 647. Solid grey curve: cells expressing GFP-rK_{2P}3.1-HA, cultured in 4.5 g/l glucose, stained with the isotype control; black solid line: GFP-rK_{2P}3.1-HA, 4.5 g/l glucose, anti-HA; black dashed line: GFP-rK_{2P}3.1-HA, 1.0 g/l glucose anti-HA; grey solid line: GFP-rK_{2P}3.1_{N53Q}HA, 4.5 g/l glucose, anti-HA; grey dashed line: GFP-rK_{2P}3.1_{N53Q}HA, 1.0 g/l glucose, anti-HA. **B**: Confocal microscopic *z*-stack images of the COS-7 cells described in panel A, fixed and stained against HA tag (red). WT: GFP-rK_{2P}3.1-HA; N53Q: GFP-rK_{2P}3.1_{N53Q}HA (green fluorescence). Merge: superimposed images of total channel expression (green) and surface-exposed HA-tag (red). Scale bar represents 10 μm.

Figure 4

rK_{2P}9.1 cell surface expression is less sensitive than rK_{2P}3.1 to channel glycosylation state. A: Currents evoked by applied membrane potential pulses from -100 to +90 mV in HEK293 cells expressing rK_{2P}9.1 (WT) or rK_{2P}9.1_{N53Q} (N53Q) at pH 7.8. B: Average current-voltage relationship for untransfected (UT) HEK293 cells, or HEK cells expressing rK_{2P}9.1 (WT) or rK_{2P}9.1_{N53Q} (N53Q) at pH 7.8. C: Flow cytometric analysis of intact COS-7 cells expressing GFP-rK_{2P}9.1-HA (WT) or GFP-rK_{2P}9.1_{N53Q}HA (HA). Cells were stained with either a monoclonal antibody against the external HA-tag, or an isotype control antibody, followed by goat anti-mouse F(ab')₂ fragment conjugated to Alexa Fluor 647. Solid grey curve: cells expressing GFP-rK_{2P}9.1-HA, stained with the isotype control. Solid black line: cells expressing GFP-rK_{2P}9.1-HA, stained with anti-HA-tag antibody. Solid grey line: GFP-rK_{2P}9.1_{N53Q}HA, anti-HA-tag. Dashed grey line: GFP-rK_{2P}9.1_{N53Q}HA, isotype control. Bar chart: summary of three independent experiments to determine the surface expression of GFP-rK_{2P}9.1_{N53Q}HA (N53Q) to GFP-rK_{2P}9.1-HA (WT). Results are expressed relative to WT (100%); error bar is S.E.M.

D: Immunofluorescence images of the COS-7 cells described above, fixed and stained to detect external HA-tag (red fluorescence). Upper panels: GFP-rK_{2P}9.1-HA; lower panels: GFP-rK_{2P}9.1_{N53Q}HA (green fluorescence). Merge: superimposed images of channel and HA-tag fluorescence. Scale bar represents 10 μm.

Sub-cellular localisation of GFP-tagged $rK_{2P}3.1$ and $rK_{2P}3.1_{N530}$

A: COS-7 cells expressing GFP-r $K_{2P}3.1$ (upper panels, WT, green) or GFP-r $K_{2P}3.1_{N53Q}$ (lower panels, N53Q, green) were fixed and stained with antibodies against 58 kDa Golgi complex protein (Golgi, red). Merge: superimposed channel and Golgi complex images. Images are single confocal sections. White bar represents 10 μ m. Transects in the Merge images (yellow) reveal the extent of co-localisation of channel and the Golgi complex signals, as both signal intensities across the length of each transect is plotted in the graphs to the right of the confocal images.

B: As **A**, but cells were stained with an antibody against ERGIC-53.

Figure 6

Is reduced function of glycosylation mutant $rK_{2P}3.1_{N53O}$ due to lower channel stability?

A: Flow cytometric analysis of COS-7 cells expressing GFP-rK_{2P}3.1-HA without (solid black line) and in the presence of 1 μg/ml tunicamycin (dashed black line), or GFP-rK_{2P}3.1_{N53Q}HA without (solid grey line) or with tunicamycin (dashed grey line). The population of GFP-positive cells is denoted by 'Transfected cells', derived by comparing to cells transfected with empty vector alone (data not shown). **B upper panels**: confocal microscopic images of COS-7 cells transfected with GFP-rK_{2P}3.1 (WT, green), surface biotinylated (Biotin, red), then allowed to endocytose for 20 min before fixing and staining with anti-EEA1 (EEA1, blue). Merge: superimposed images of channel, biotin and EEA1. Examples of triple-stained vesicles are denoted with white arrows and numbers correspond to transects (transects themselves not shown on the Merge image), which appear in the **lower panels 1-4**, as graphs of fluorescence intensity against distance. White scale bar represents 10 μm. **C**: As described for **B**, except cells express GFP-rK_{2P}3.1_{N53Q} (N53Q, green).

Table 1.

| Channel | Name | Tag | Mutation | Experiments | | |
|---|--|------------------------|-------------------|--|--|--|
| | rK _{2P} 3.1 rK _{2P} 3.1 _{N53Q} | None None | Wild-type N53Q | Electrophysiology | | |
| K _{2P} 3.1 rat | GFP-rK _{2P} 3.1 GFP-rK _{2P} 3.1 _{N53Q} | eGFP eGFP | Wild-type N53Q | Immunofluorescence | | |
| | GFP-rK _{2P} 3.1-HA GFP-rK _{2P} 3.1 _{N53Q} HA | eGFP & HA eGFP & HA | Wild-type N53Q | Immunofluorescence; flow cytometry; immunoblotting | | |
| | rK _{2P} 9.1 rK _{2P} 9.1 _{N53Q} | None None | Wild-type N53Q | Electrophysiology Immunofluorescence Immunofluorescence; flow cytometry; immunoblotting an HA epitope tag in the Downloaded from www.jbc.org at University of Southampton Libraries, on January 31, 2013 | | |
| K _{2P} 9.1 rat | GFP-rK _{2P} 9.1 GFP-rK _{2P} 9.1 _{N53Q} | eGFP eGFP | Wild-type N53Q | Immunofluorescence | | |
| | GFP-rK _{2P} 9.1-HA GFP-rK _{2P} 9.1 _{N53Q} HA | eGFP & HA eGFP & HA | Wild-type N53Q | Immunofluorescence; flow cytometry; immunoblotting | | |
| Table 1 Summary of K_{2P} constructs used in this study Channels were tagged with eGFP fused to the N-terminus, with or without an HA epitope tag in the external loop of the second pore-forming domain. | | | | | | |

Table 2.

| Channel | Human | Mouse | Rat |
|-------------------------------|----------|----------|----------|
| K _{2P} 1.1 (TWIK-1) | N95 | N95 | N95 |
| K _{2P} 2.1 (TREK-1) | N110 | N110 | N95 |
| | N134 | N134 | N119 |
| K _{2P} 3.1 (TASK-1) | N53 | N53 | N53 |
| K _{2P} 4.1 (TRAAK) | N78 | | |
| | N82 | N81 | N81 |
| K _{2P} 5.1 (TASK-2) | N77 | N77 | N77 |
| K _{2P} 6.1 (TWIK-2) | N85 | N83 | N79 |
| | | | N85 |
| $K_{2P}7.1$ | N83 | | N83 |
| K _{2P} 9.1 (TASK-3) | N53 | N53 | N53 |
| K _{2P} 10.1 (TREK-2) | N144 | N144 | |
| | N148 | N148 | |
| K _{2P} 12.1 (THIK-2) | N78 | N78 | N78 |
| K _{2P} 13.1 (THIK-1) | N59 | N59 | N59 |
| | N65 | N65 | N65 |
| K _{2P} 15.1 (TASK-5) | No sites | No sites | No sites |
| K _{2P} 16.1 (TALK-1) | N57 | N57 | N57 |
| | N86 | N86 | N86 |
| K _{2P} 17.1 (TALK-2) | N65 | | |
| | N94 | | |
| K _{2P} 18.1 (TRESK) | N70 | | |
| T.11.2 D. H. J.V. | N96* | N94 | N83 |

Table 2 *Predicted N-glycosylation sites in* K_{2P} *channels*

Protein sequences were analysed using the NetNGlyc Server 1.0, hosted by the Center for Biological Sequence Analysis at the Danish Technical University. *This site is predicted, but only N70 is glycosylated in human $K_{2P}18.1$ [27].

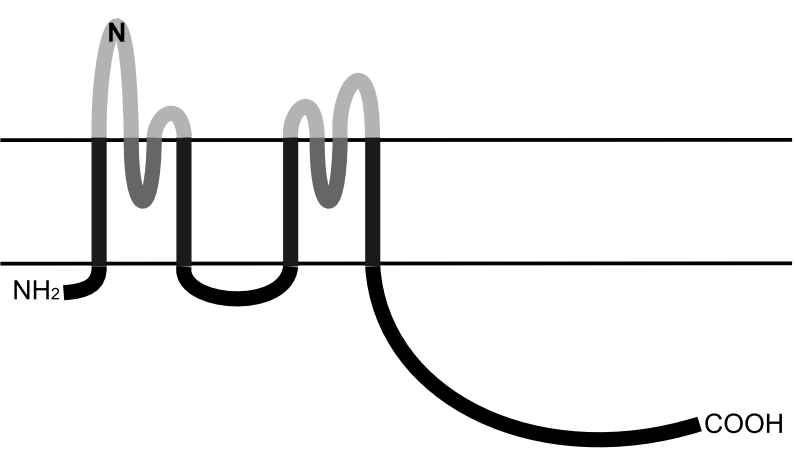
Α

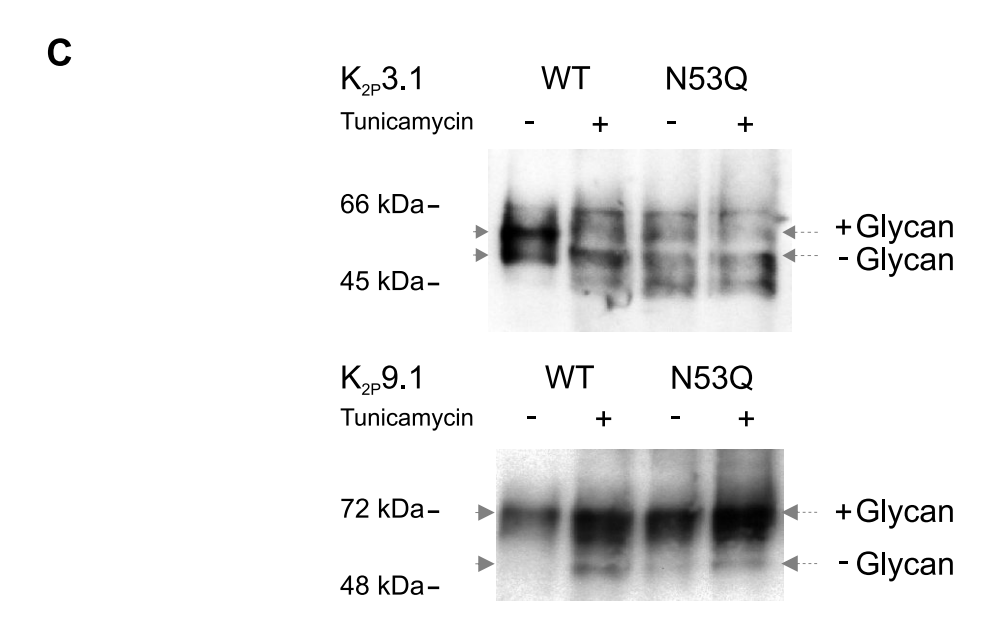


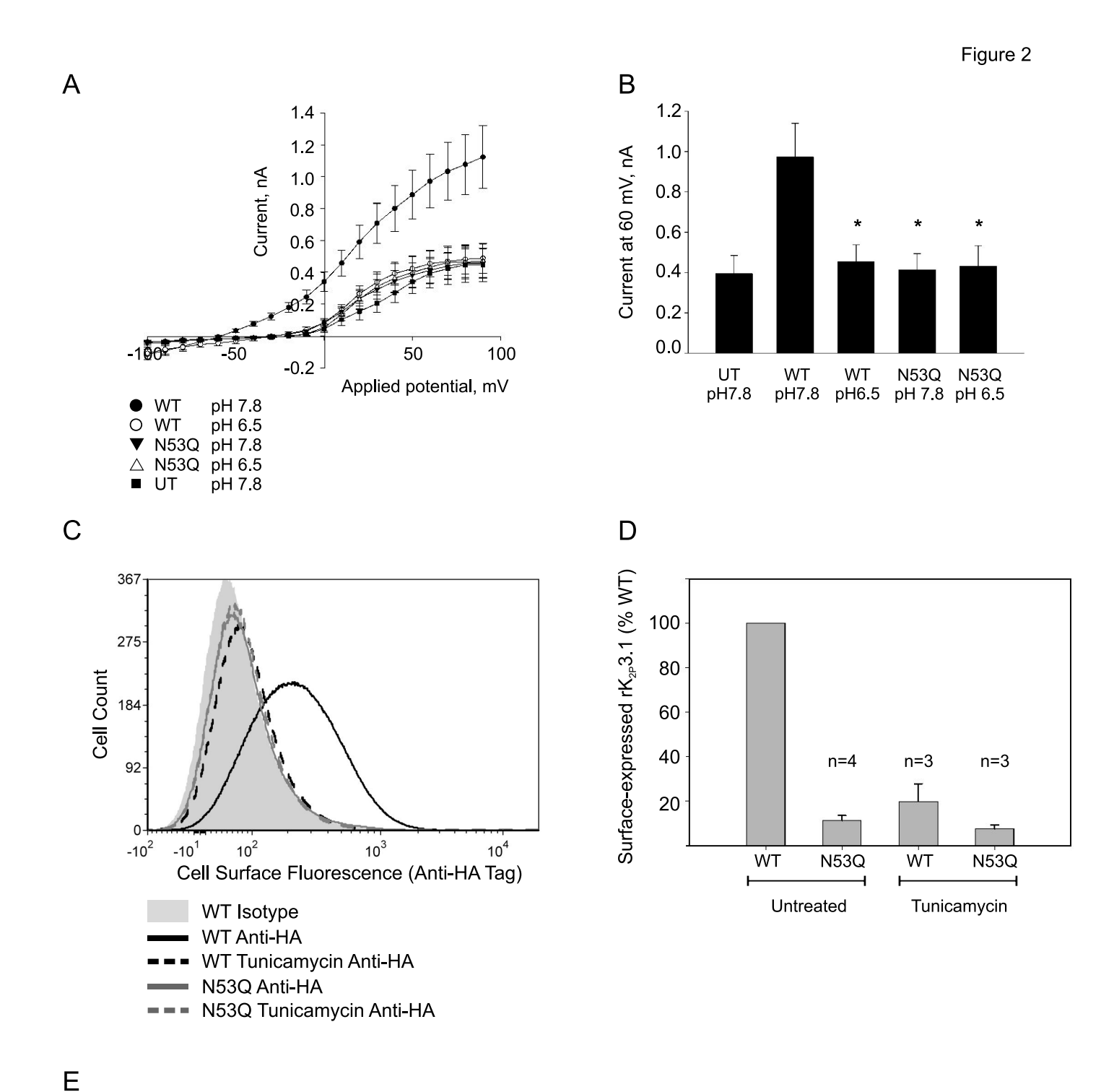
N-glycosylation consensus sequence

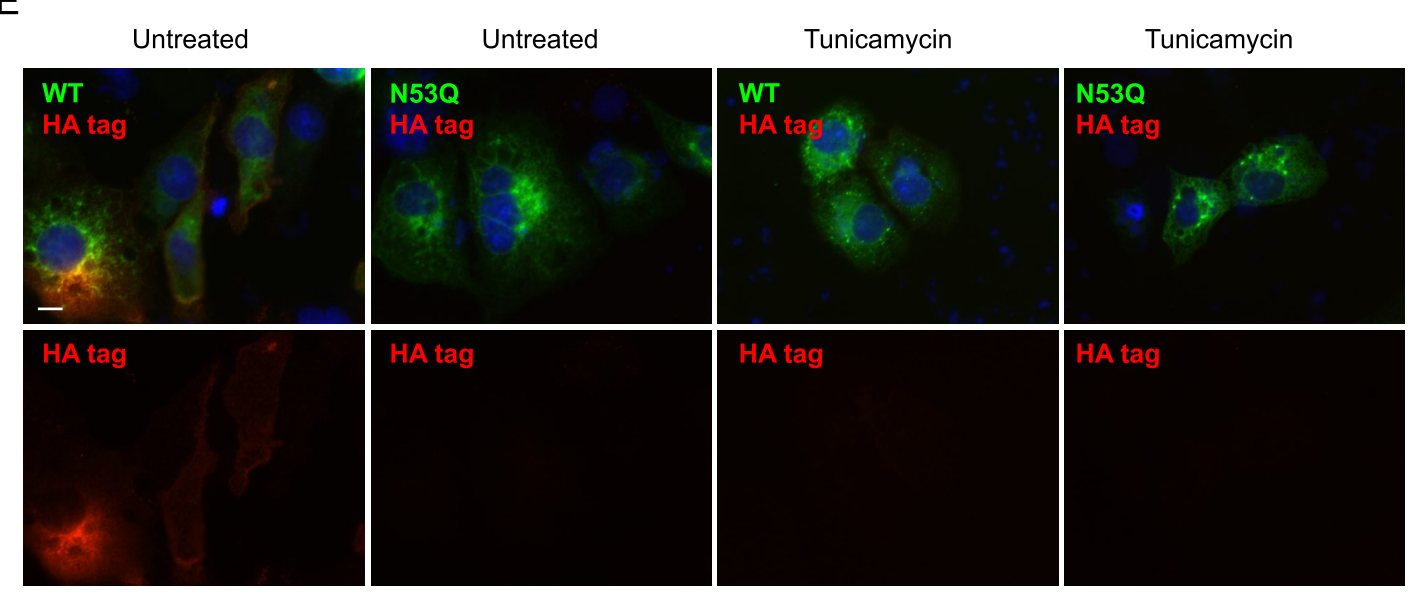
selectivity pore consensus sequence



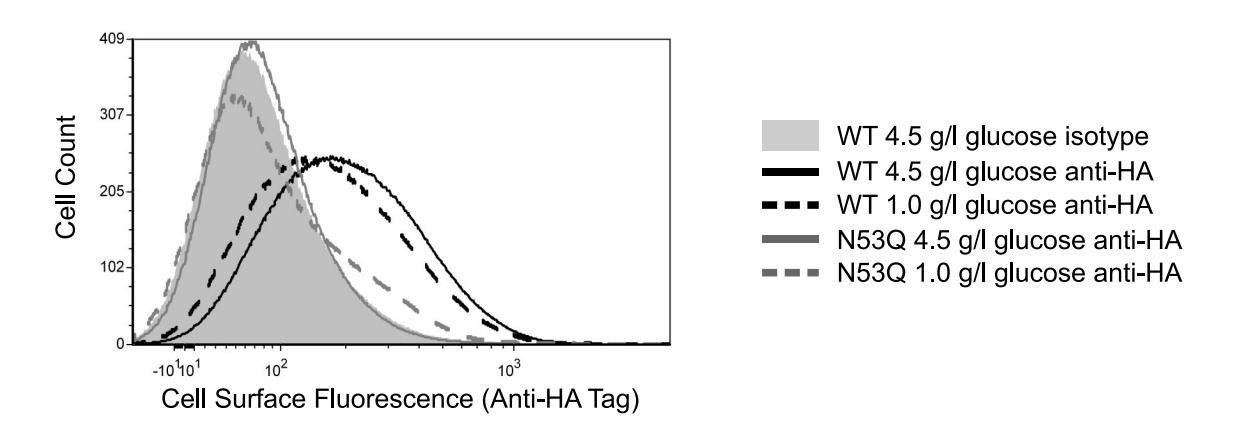




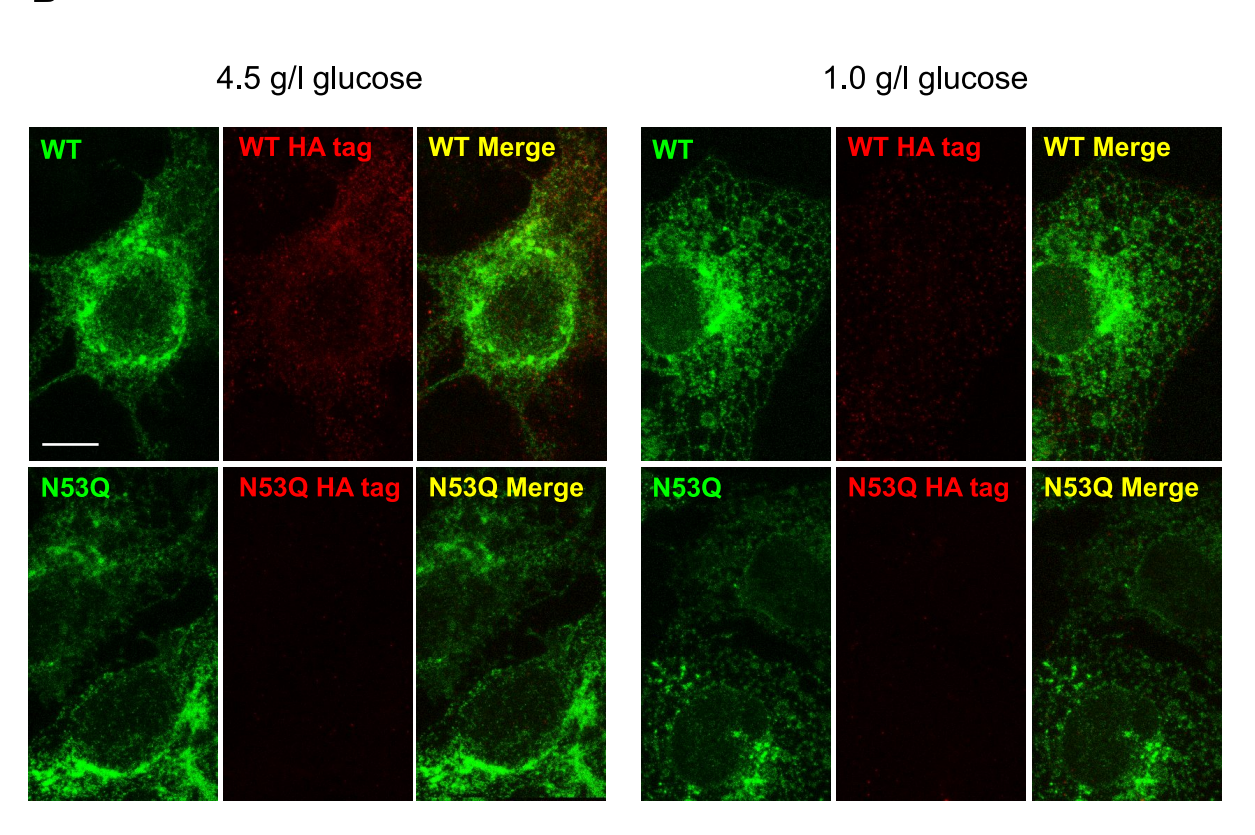


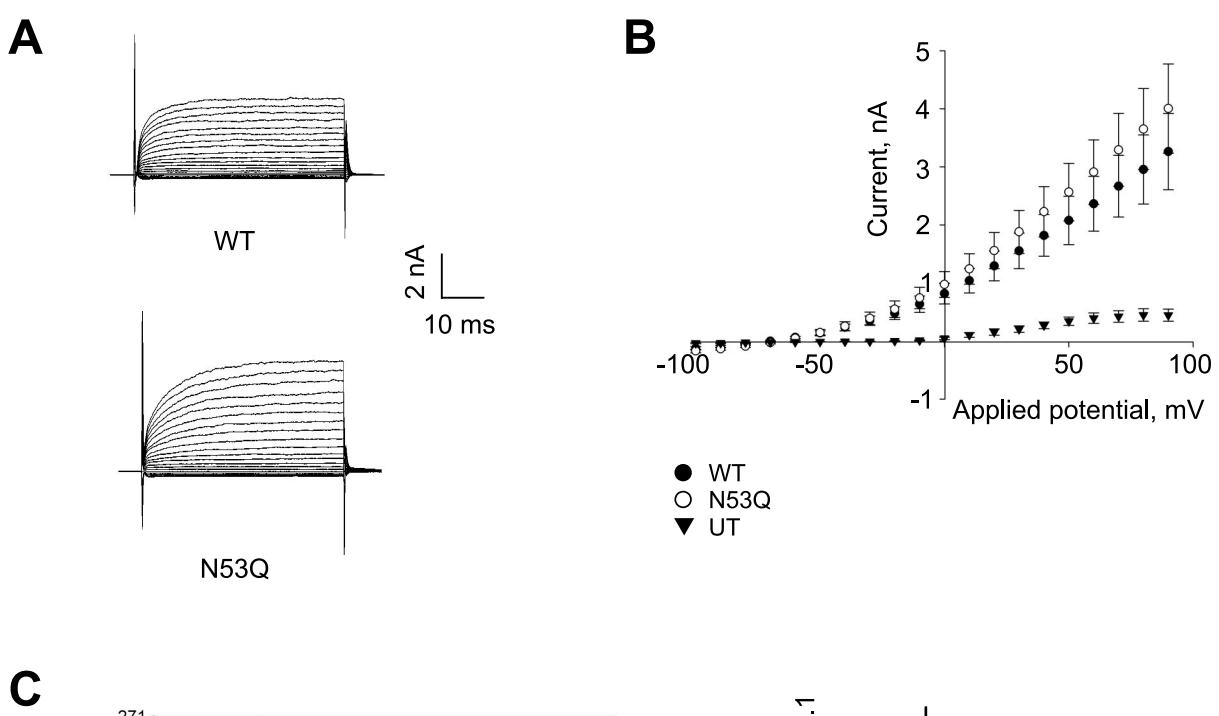


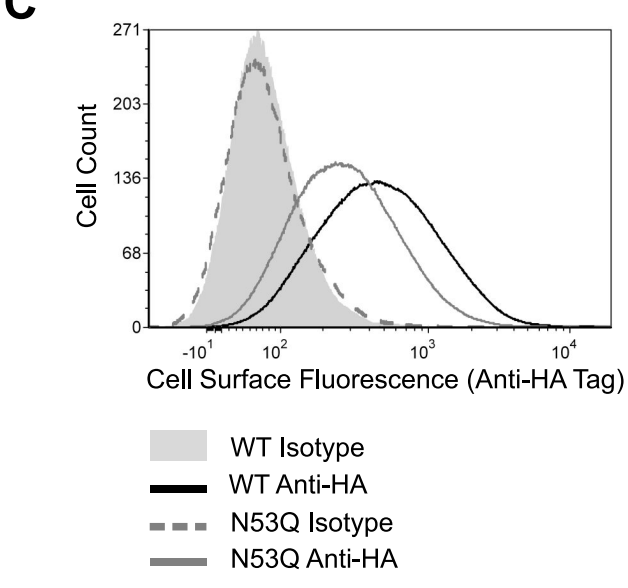


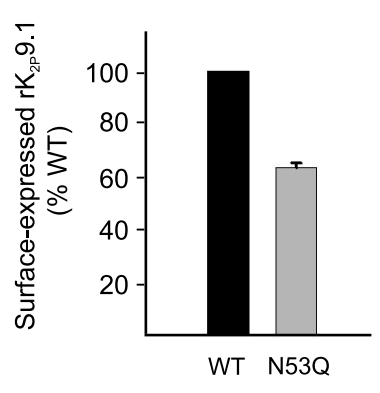


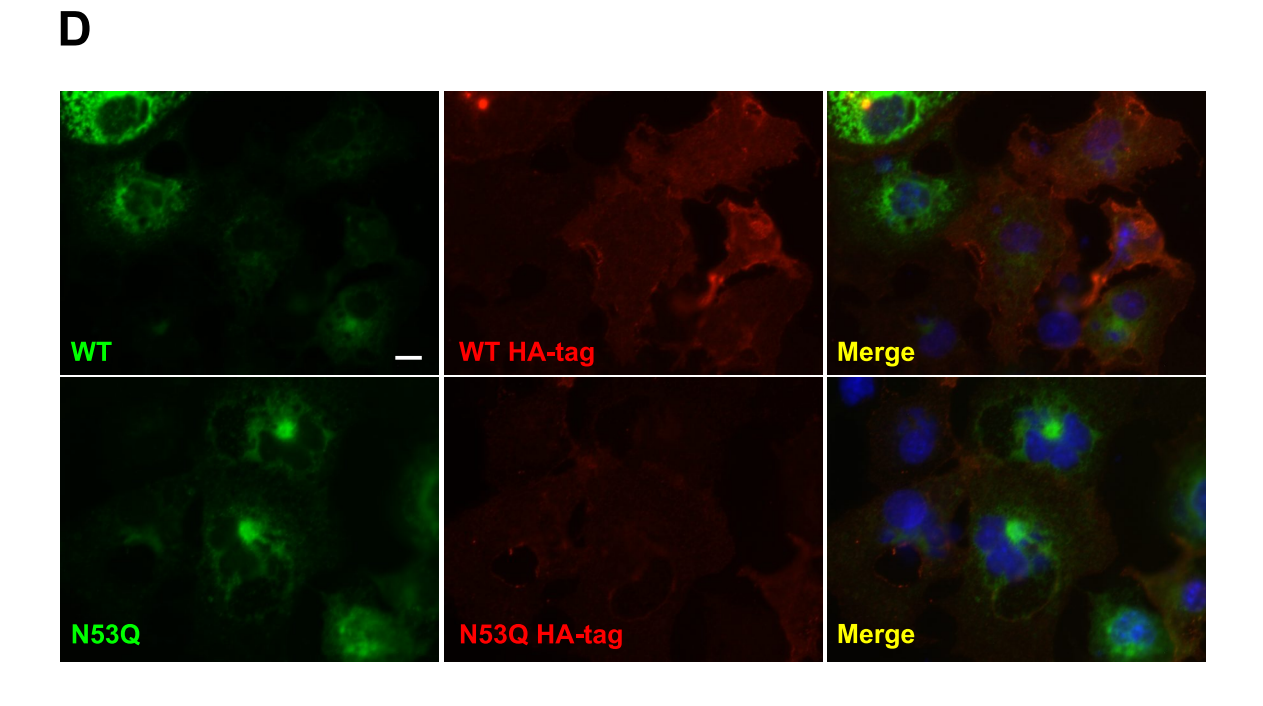
В

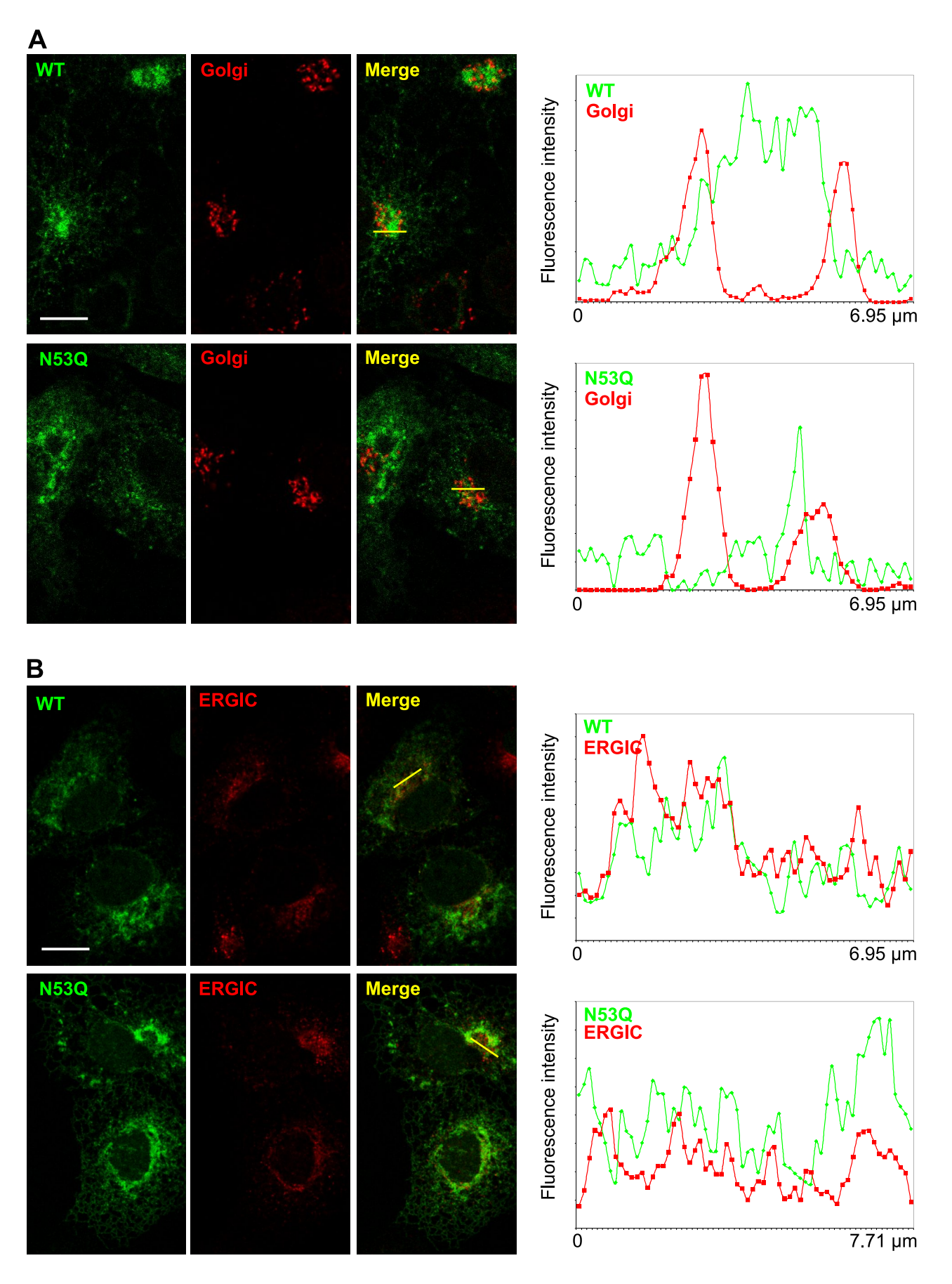




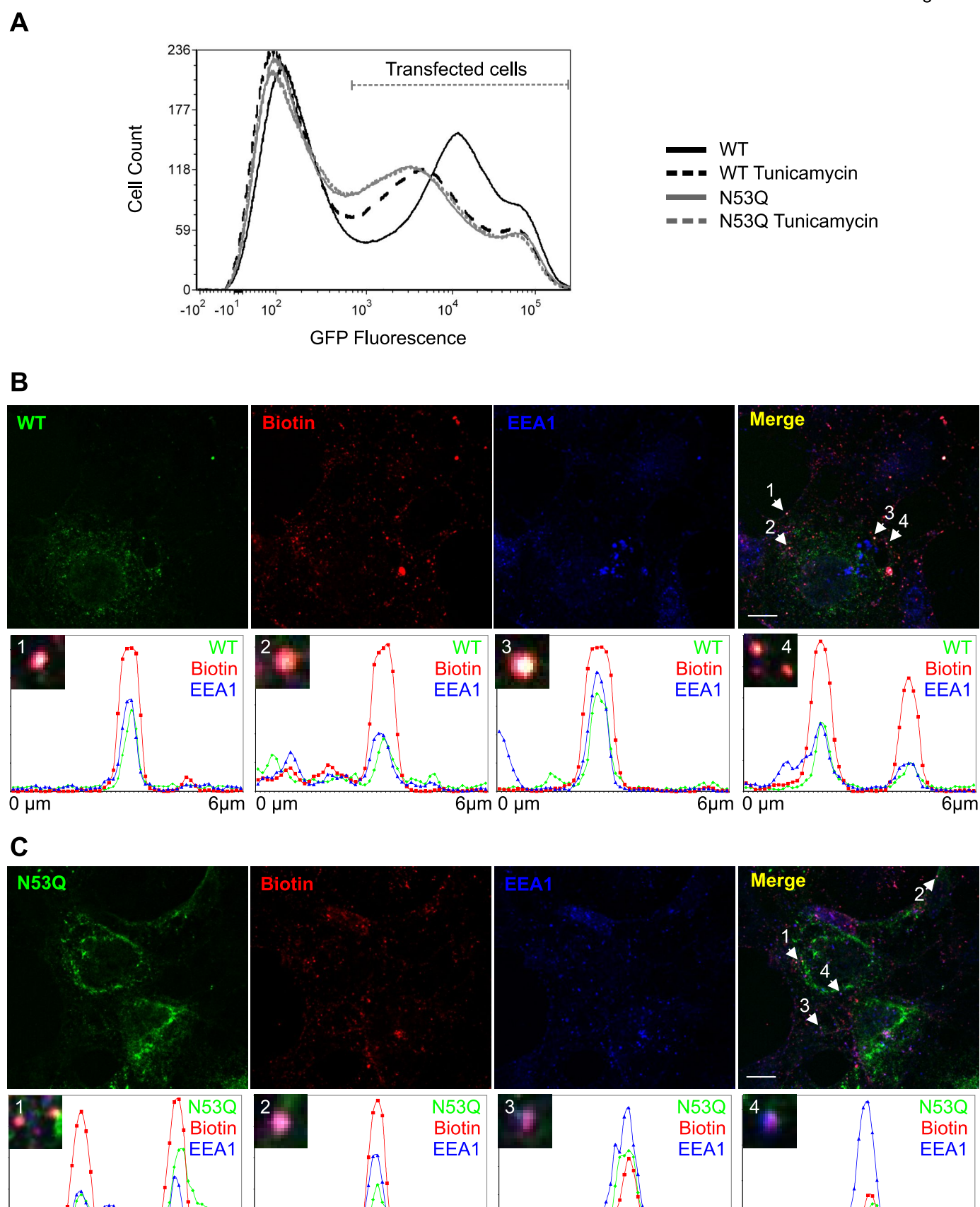








6µm



6μm 0 μm

6μm 0 μm

6µm 0 µm

0 µm